EMITTANCE MEASUREMENT PROCEDURES FOR THE SwissFEL 250 MeV INJECTOR

Bolko Beutner
Paul Scherrer Institut, 5232 Villigen PSI, Switzerland

Abstract

The planned SwissFEL facility will supply coherent, ultra-bright, and ultra-short x-ray beams covering a wide wavelength range from 0.1 nm to 7 nm, with nominal electron beam emittances in the range from 0.18 to 0.43 mm mrad at the undulator entrance. At the 250 MeV Injector test facility the beam quality will be studied to confirm the feasibility of the SwissFEL project requirements. In order to understand and optimise the electron beam, precise measurements of the beam properties are essential. We discuss here a diagnostics setup consisting a 3.5-cell FODO lattice, and includes a transverse deflecting rf structure for longitudinally resolved measurements. In this paper the techniques for emittance and Twiss parameter reconstruction are discussed. The layout of the diagnostic optics setup and the strategy for measurements of the emittance are presented. Data on the systematic error concerning beam size measurement and beam energy uncertainties complete this summary.

INTRODUCTION

One part of the mission of the 250 MeV Injector test facility is to demonstrate the production and transport of low emittance beams including bunch compression and beam matching into FODO linac structures [1]. For this purpose a diagnostic FODO section has been designed to establish the required parameters. Experience in FODO emittance measurements, e.g., from FLASH is used for this study [2].

Emittance Measurements

Emittance reconstruction is based on a fit of the beam moments to the beam sizes for different positions in the beamline using the transport matrices $R^{(i)}$ (compare [2],[3]).

From the measured beam sizes the variance $< x^2_{(i)} >$ and their errors $\sigma_{<x^2_{(i)}>}$ are derived. The theoretical beam size square from the beam moments at a reference position $< x_0^2 >$, $< x_0 x_0' >$, and $< {x_0'}^2 >$

$$f_i = R_{11}^{(i)\,2} < x_0^2 > + 2R_{11}^{(i)} R_{12}^{(i)} < x_0 x_0' > + R_{22}^{(i)\,2} < {x_0'}^2 >, \quad (1)$$

can be obtained using a χ^2-optimisation of

$$\chi^2 = \sum_{i=1}^{n} \left[\left(\frac{< x^2_{(i)} > - f_i}{\sigma_{<x^2_{(i)}>}} \right) \right]^2 \quad (2)$$

with n being the number of the beam size measurements. From these beam moments the Twiss parameters and the emittance are determined.

Diagnostic Section

A description and functional layout of the 250 MeV Injector is presented in [1]. The optics layout of the beam diagnostics section for the 250 MeV Injector is shown in Fig. 1. The main feature of the FODO section is that the beam energy errors are automatically canceled for the determination of normalised beam emittance [4]. In this paper

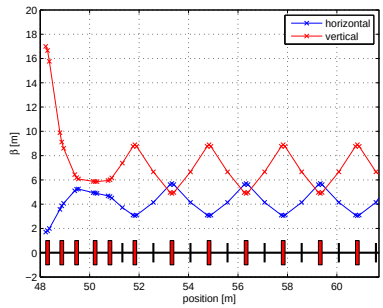

Figure 1: Optics layout of the 250 MeV Injector's diagnostic section. The first five quadrupoles (left) match the beam from the transverse deflecting cavity to the diagnostic FODO channel (right). Screens are indicated as black lines and quadrupoles are represented by red boxes.

an FODO lattice with different phase advances in the both planes is discussed, which consists of 3.5 FODO cells with phase advances of 42° and 26° in the horizontal and vertical plane, respectively. The beta functions on the screen are 4.2 m and 6.7 m in the two planes. This setup is designed for horizontal slice emittance measurements using a vertical rf deflector. The phase advance in the horizontal plane is optimised to cover enough phase advance for emittance measurements, while the vertical phase advance allows for a good longitudinal resolution for the vertical deflector measurements. As we will see later this asymmetric lattice is not optimal for vertical emittance measurements. For projected emittance measurements we symmetrise the lattice with identical phase advances in both planes. The results of our discussion remain valid if the phase advance in the symmetric configuration matches that in the horizontal plane in the asymmetric lattice. The beam-size based measurement technique presented above is suitable for projected and slice emittance measurements. The main dif-

ference is the determination of the beam size for the corresponding longitudinal slices in the image analysis. The assumption of larger assumed errors in the beam size measurement can reflect this additional complication.

IMAGE ANALYSIS

The proper determination of beam size is critical for the emittance determination. This can be done by wire scanners or screens. In both cases a problem arises from the noise. This can be pixel noise from the CCD readout or noise on the photomultipliers from the wirescanners. A standard technique is to fit a Gaussian to the beam profile, using the σ as the beam size. This works relatively well but is only well defined if the beam has a roughly Gaussian shape. For stronger noise contributions a Gaussian fit to the beam is not always successful. For arbitrary beam profiles one should use the rms beam size. However, the rms beam size is particulary affected by noise, since "hot pixels" far away from the beam centre of mass will dominate the evaluated rms value. To deal with the noise an

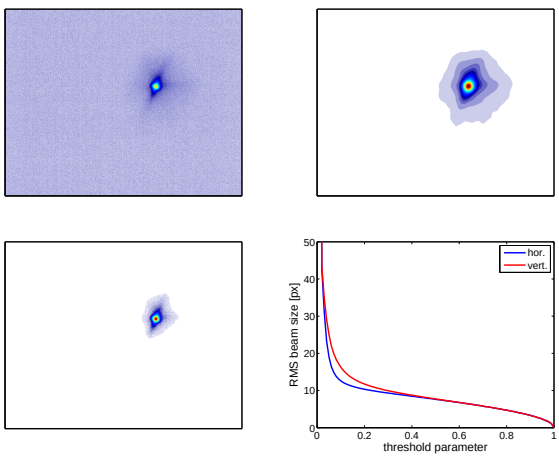

Figure 2: Overview of the noise cut image analysis. A beam image taken from a solenoid scan at OBLA 4 MeV [5] contains noise (top left). A smoothed image (top right). Original image after threshold cut with a threshold parameter of 0.04 (bottom left). RMS beam size as a function of threshold parameter (bottom right).

"adaptive region of interest" procedure is used (as shown in Fig. 2). The original image is first smoothed with a standard 2D Gaussian convolution. The effect is that the beam is smeared out, increasing the beam size, while the noise is substantially reduced. This smoothed image is now compared with a threshold parameter. It is defined as a number between 0 and 1, corresponding to the minimum and maximum pixel intensity, respectively. All pixels of the smoothed image below that threshold are considered to be part of the "background" and not beam related. All pixels above that threshold represent the "beam". This set of the "background" pixels, as obtained from the smoothed image, is then considered as background in the original image as well. We consider the mean pixel intensity of the "background" area as the pedestal value of the image and subtract this value from the raw image. As a final step we set all pixels, belonging to the "background" area to zero as shown in Fig. 2 (bottom left). This processed original image is now used for the determination of the rms size. Since noise pixels outside the beam domain are set to zero their effect on the rms beam size is removed. The whole procedure depends on the choice of the threshold parameter. To get a reasonable value for the threshold parameter the rms beam size is evaluated as a function of the threshold parameter (compare Fig. 2, bottom right). Values toward unity will cut parts of the beam eventually resulting in a rms size of zero. Threshold parameters close to one will spare parts of the background so that their rms size will be dominated by the noisy pixels far outside. In between, however, the rms beam size is not changing dramatically. In a semi-automatic procedure a threshold parameter inside the stable region is chosen. For emittance measurements in a FODO section a relatively stable beam size and shape can be assumed so that this threshold parameter calibration has to be done only occasionally. For solenoid or quadrupole scans the threshold calibration has to be redone for every significant beam shape change. There is no restriction in using the described procedure for 1D data like wirescans. This image processing procedure has already been successfully tested and applied for solenoid- and slit-scans at the OBLA 4 MeV Gun test facility [5].

SYSTEMATIC ERRORS

Measurement errors on the beam size, including image analysis, and inaccuracies in the transport matrices, used for the emittance reconstruction, are the main error sources for emittance measurements. Here systematic uncertainties in the beam lattice matrices are studied – this is not a jitter study!

The assumed transport matrices can be wrong if either the energy is not known exactly or the quadrupole magnet fields calibrations are not correct. Since we are using a FODO channel for emittance measurements a strong impact could be expected if one deviates from the periodic solution. The effect of a possible mismatched beam is studied. To study beam mismatch it is convenient to introduce the mismatch parameter

$$\xi = \frac{1}{2}\left(\beta\gamma_0 - 2\alpha\alpha_0 + \gamma\beta_0\right), \qquad (3)$$

with $(\alpha_0, \beta_0, \gamma_0)$ being the design Twiss parameters and (α, β, γ) the actual ones. For a perfect matched beam the mismatch factor is $\xi = 1$. In the following we study how the accuracy of emittance measurements is affected by beam size errors.

Beam Size Errors

Figure 3 displays the summary of a Monte Carlo study concerning a beam mismatch. Here and in the following

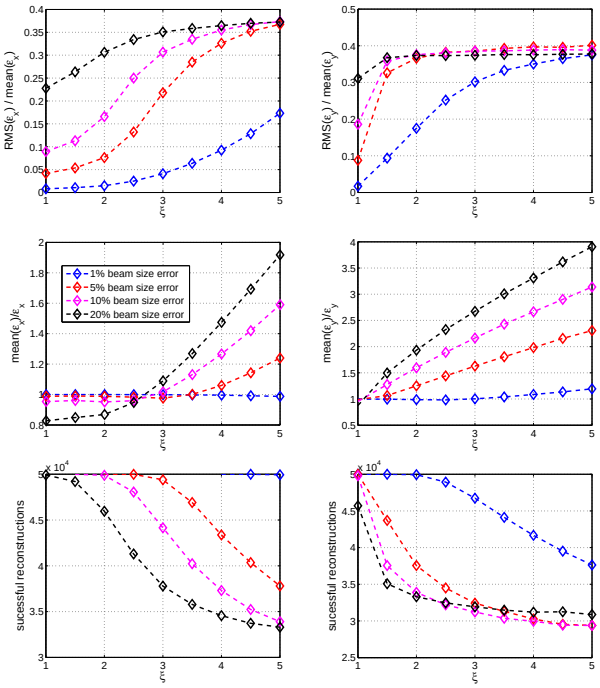

Figure 3: Results of a Monte Carlo study for beam size errors with induced mismatch ξ for the horizontal (left) and vertical (right) plane. Top line: relative emittance RMS variation. Centre line: comparison with the original normalised emittance ($\varepsilon_x = \varepsilon_y = 0.4$ mm mrad). Bottom line: number of successful phase space fits. Note that the discussed lattice is not optimised for vertical but for horizontal slice emittance measurements.

calculations matrix tracking is used to obtain theoretical beam size values, which are then modified according to assumed errors. The α parameter is modified according to

$$\alpha = \alpha_0 - \sqrt{2\xi - 2}, \tag{4}$$

with the beam mismatch parameter ξ, while β is kept constant and γ adjusted accordingly. Such a well defined mismatch parameter ξ is used to study the effect of beam size errors. A set of 50,000 random beam sizes (normally distributed around the theoretical value with different assumed σ's) for every screen in the FODO section is generated assuming a normalized emittance of 0.4 mm mrad in the horizontal and vertical plane, for every induced beam mismatch. The relative emittance error (Fig. 3 top) for these data, the average deviation of the reconstructed value to the original one (Fig. 3 centre), and the number of successful emittance reconstructions (Fig. 3 bottom) is shown for both the horizontal and vertical phase space. In the horizontal plane the emittance measurements have reasonably small errors up to about $\xi = 2$. In the vertical plane, were a much smaller phase advance is covered, a reasonable measurement is possible almost only for the matched solution. For small beam mismatch parameters the emittance in the horizontal plane is slightly underestimated. For a large mismatch in the horizontal and always in the vertical plane, the emittance is roughly linearly overestimated with the mismatch parameter (Fig. 3 centre). For high beam mismatch parameters or large beam size measurement errors only a fraction down to 60% of the attempts to reconstruct the beam moments were successful (no real solution). The optics is designed for slice emittance measurements in the horizontal plane, therefore the phase advance in the vertical plane is not sufficient for good emittance measurement in the vertical plane. Recall that a symmetric FODO lattice is used for projected emittance and beam matching measurements which gives a performance similar to the horizontal case. In the following we will discuss only the errors in the horizontal plane, which give the numbers relevant for a symmetric lattice.

In standard operation of the machine, mismatch parameters are expected very close to unity. However, it is important to design the diagnostic section to handle large mismatch parameters to obtain a reasonable matching to the periodic solution in the first place. The behaviour of the Twiss parameters is very similar to the emittance. For the beam matching in the machine one will start with a mismatched beam, and therefore the measured Twiss parameters, which are used for the quadrupole correction calculation, are slightly wrong. An iterative process is needed to obtain good matching. If the measurements are too inaccurate for large beam mismatch one will have a slow or (in the worst case) no convergence. The experience, e.g., from FLASH shows that typically 2–4 iterations are required. An important remark is that it is not straightforward to define a beam size error as a simple percentage of beam size, it is actually beam size dependent. For small beam sizes the optical resolution of the camera system plays a role, while for large beam spots the readout noise from the CCD affects the measurement. A study on this behaviour is beyond the scope of this paper. The data presented here are still valid but one has to keep in mind that the beam size error is not constant as assumed for this study.

Mismatch Maps

The induced beam mismatch used in the last section is a special case, since in general the beam mismatch will deviate from Eq. 4. Error propagation is used to determine the expected error for different initial optics parameters in the FODO section. In Fig. 4 (left) the error calculated from the error propagation for different assumed beam size errors as a function of the optics parameters (β, α) in the FODO channel are shown. Values over 20% are set to 20% in order to make small errors visible in the colour map. As a result it is seen that a big mismatch can, for the right optics configuration (e.g., high β and small α), still be used for reasonable measurements with small errors. In case of a beam matched to the periodic solution one gets an error as a function of the assumed beam size error. This is shown in Fig. 4 (right), to estimate the required beam size measurement accuracy for a certain emittance determination precision.

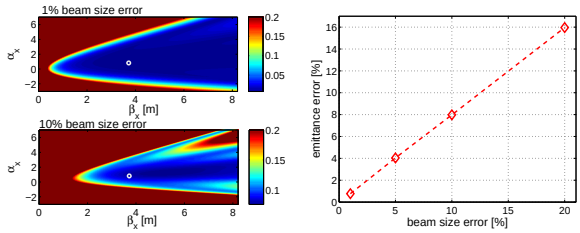

Figure 4: Error calculated from error propagation of the emittance fit for different initial optics (β, α) in the FODO channel for different assumed beam size errors in a colour code (left). Errors are limited to 20%. The periodic solution of the FODO channel is indicated by a white circle. The emittance error for the periodic solution depends almost linearly on beam size error (right).

Energy Errors

Uncertainties in the beam energy and the corresponding inaccuracies in the quadrupole focussing strength are studied with Monte Carlo methods. From theory the errors of the normalised emittance are expected to be independent of energy mismatch [4], while higher order contributions still remain. The beam optics is varied. For each optics configuration 100 random energies with a certain assumed energy error are diced. In Fig. 5 the relative normalised emittance error is plotted as a function of beam optics parameters for assumed energy errors of 1% and 10% (left), as well as a summary of the relative normalised emittance error as a function of assumed energy error (right).

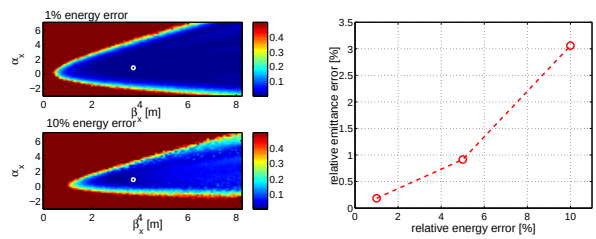

Figure 5: Errors of the reconstructed normalised emittance if an energy error is assumed. Monte Carlo study with 100 random values (assuming an energy error of 1% and 10%) for every beam optics state (β, α) (left). The periodic solution of the FODO channel is indicated by a white circle. Errors are limited to 50% in order to have the smaller errors still visible. The normalised emittance error for the periodic solution depends slightly quadratic on energy error which indicates the cancelation of the first order term (right).

Quadrupole Errors

In the previous study the effect of an uncertainty in the energy is equivalent to a systematic quadrupole calibration error. To study individual quadrupole errors a similar Monte Carlo approach is used. In this case not the beam energy but all focussing strengths in the FODO lattice are randomised. A summary of the results is displayed in Fig. 6. Comparing the relative normalised emittance error one sees a bigger contribution from the individual quadrupole error than for the energy error. In the FODO lattice with energy errors the solution is still periodic while this is not the case for individual quadrupole errors. Therefore only higher orders play a role for the energy errors, while the behaviour of the errors is dominated by the linear first-order contributions from individual quadrupole field errors.

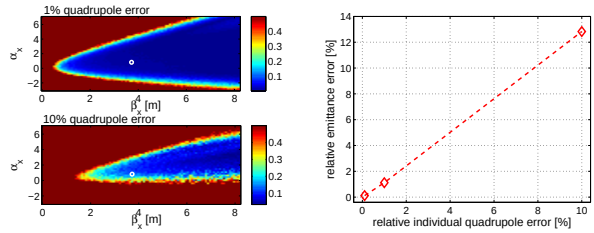

Figure 6: As in Fig. 5 but errors caused by individual quadrupole errors are studied. The emittance error for the periodic solution depend almost linearly on the quadrupole strength error (right).

CONCLUSION

The proposed diagnostic FODO section at the 250 MeV injector is a powerful tool for emittance measurements. In this paper, it was shown that emittance measurements and beam matching measurements are possible within reasonable error bounds. Furthermore systematic errors were estimated. To achieve 5% relative normalised emittance error a beam size accuracy of 6%, an energy error of more than 10%, or an individual relative quadrupole error of 4% are tolerable.

ACKNOWLEDGEMENTS

Valuable contributions and fruitful discussions for this paper from Rasmus Ischebeck, Anne Oppelt, Sven Reiche, and Yujong Kim are acknowledged.

REFERENCES

[1] M. Pedrozzi, Proceedings of FEL'09 Conference, Liverpool, August 2009.

[2] F. Löhl, "Measurement of the Transverse Emittance at the VUV-FEL", Master Thesis (Diplomarbeit), University of Hamburg, 2005

[3] M. Minty and F. Zimmermann, "Measurements and Control of Charged Particle Beams", Springer, Berlin, Heidelberg, New York, 2003.

[4] P. Castro, "Monte Carlo Simulations of Emittance Measurements at TTF2", DESY Technical-Note-2003-03, 2003.

[5] R. Ganter, Proceedings of FEL'09 Conference, Liverpool, August 2009.